PLOS ONE

RESEARCH ARTICLE

Hyperuricaemic *Urah*$^{Plt2/Plt2}$ mice show altered T cell proliferation and defective tumor immunity after local immunotherapy with Poly I:C

Camille Baey, Jianping Yang, Franca Ronchese*, Jacquie L. Harper

Malaghan Institute of Medical Research, Wellington, New Zealand

These authors contributed equally to this work.
* fronchese@malaghan.org.nz

Check for updates

OPEN ACCESS

Citation: Baey C, Yang J, Ronchese F, Harper JL (2018) Hyperuricaemic *Urah*$^{Plt2/Plt2}$ mice show altered T cell proliferation and defective tumor immunity after local immunotherapy with Poly I:C. PLoS ONE 13(11): e0206827. https://doi.org/10.1371/journal.pone.0206827

Editor: Michal A. Olszewski, University of Michigan Health System, UNITED STATES

Received: January 18, 2018

Accepted: October 19, 2018

Published: November 1, 2018

Copyright: © 2018 Baey et al. This is an open access article distributed under the terms of the Creative Commons Attribution License, which permits unrestricted use, distribution, and reproduction in any medium, provided the original author and source are credited.

Data Availability Statement: All data from this study are available in the Figures in the manuscript itself, and as part of the supplemental information.

Funding: This work was funded from Project grant 14-285 from the Health Research Council of New Zealand (http://www.hrc.govt.nz) to FR and JH. The funders had no role in study design, data collection and analysis, decision to publish, or preparation of the manuscript.

Competing interests: The authors have declared that no competing interests exist.

Abstract

Hyperuricaemia is associated with various metabolic dysfunctions including obesity, type 2 diabetes mellitus, hypertension and in general metabolic syndrome, which are all associated with increased risk of cancer. However, the direct association between elevated uricemia and cancer mortality still remains unclear. In this study, we used a mouse model of hyperuricemia, the *Urah*$^{plt2/plt2}$ (PLT2) mouse, to investigate the effect of high uric acid levels on anti-tumor immune responses and tumor growth. In normo-uricaemic C57BL/6 mice injected with B16 melanomas, immunotherapy by treatment with Poly I:C at the tumor site delayed tumor growth compared to PBS treatment. In contrast, Poly I:C-treated hyper-uricaemic PLT2 mice were unable to delay tumor growth. Conventional and monocyte-derived dendritic cells in the tumor-draining lymph nodes (dLN) of C57BL/6 and PLT2 mice were similarly increased after Poly I:C immunotherapy, and expressed high levels of CD40 and CD86. CD8$^+$ T cells in the tumor-dLN and tumor of both WT and PLT2 mice were also increased after Poly I:C immunotherapy, and were able to secrete increased IFNγ upon *in vitro* restimulation. Surprisingly, tumor-specific CD8$^+$ T cells in dLN were less abundant in PLT2 mice compared to C57BL/6, but showed a greater ability to proliferate even in the absence of cognate antigen. These data suggest that hyperuricaemia may affect the functionality of CD8$^+$ T cells *in vivo*, leading to dysregulated T cell proliferation and impaired anti-tumor activity.

Introduction

Metabolic syndrome (MS) describes the metabolic dysfunction associated with obesity and increased risk of type 2 diabetes mellitus and cardiovascular diseases. The alarming increase in MS has become a major health concern internationally. These concerns arise not only from the life-threatening nature of the MS itself but are also due to the negative impact it has on other diseases including cancer [1–3]. Latterly, there is a growing body of epidemiological data

that shows a strong link between MS and a number of different cancers in both men and women, ranging from colorectal [4, 5] through to prostate [6] and breast cancers [7, 8].

The multifactorial nature of MS makes it difficult to determine the contribution(s) of single, or groups of, components towards the negative impact of MS on cancer [5, 9]. Nevertheless, there is evidence of links between carcinogenesis and changes in glucose and/or lipid metabolism [10, 11], as well as chronic MS-related inflammation [12, 13].

One condition commonly observed with MS is chronic hyperuricaemia—uric acid build up resulting from the dysregulation of purine metabolism and/or uric acid clearance. Most commonly known for its role in the development of gout, epidemiological studies also link hyperuricaemia with carcinogenesis [14] where gout and hyperuricaemia are both associated with both risk of cancer and poor cancer prognosis [10, 15, 16].

In vivo experimental models of MS exhibit dysfunctional purine metabolism and elevated uric acid levels [17]. As in the clinical setting, the challenge of using these models to investigate the impact of purine metabolism in conditions like cancer is the presence of confounding factors such as obesity and diabetes. Previous work looking at the interference of purine metabolism in normal weight mice provides an opportunity to investigate the association between purine metabolism and cancer in the absence of these confounding factors. The *Urah*$^{plt2/plt2}$ (PLT2) mice carrying a mutation of the *Urah* gene encoding mouse 5-hydroxyisourate hydrolase (HIU-H) show increased platelet numbers and hepatomegaly [18]. Both of these defects are rescued by expression of the intact form of the *Urah* gene, demonstrating the essential role of the *Urah*$^{plt2/plt2}$ mutation in this phenotype. In addition, as predicted on the basis of the essential function of HIU-H in urate catabolism, the *Urah*$^{plt2/plt2}$ mutation also results in perturbed purine metabolism and chronically increased uricemia without affecting body weight.

Effective anti-cancer therapies often exploit the immune system to boost anti-cancer responses by enhancing the inflammatory functions of key immune cells including antigen-presenting dendritic cells (DC) and CD8$^+$ effector T cells (reviewed in [19, 20]). A number of studies identify the crystalline form of uric acid (monosodium urate-MSU) as an effective adjuvant that can boost a variety of immune responses, and has been shown to enhance the effectiveness of anti-cancer therapies in experimental models [21, 22].

Although elevated serum uric acid has been targeted in cancer in the context of Tumor Lysis Syndrome arising as a side effect of anti-tumor therapies [23], to date there has been no focus on how a pre-existing background of altered purine metabolism might impact on cancer treatment. In this study, we utilized the PLT2 model to investigate the impact of perturbed purine metabolism on both the tumorigenesis of B16 melanoma and the effectiveness of immune-mediated anti-tumor therapy. How altered purine metabolism affected classical components linked with successful anti-cancer immune responses was also investigated, with a focus on DC phenotypes and CD8$^+$ T cell functions.

Materials and methods

Mice

All mice were bred at the Malaghan Institute of Medical Research Biomedical Research Unit and were matched for age and sex within experiments. C57BL/6J were originally from The Jackson Laboratory, Bar Harbor, ME. C57BL/6-background *Urah*$^{plt2/plt2}$ (PLT2) mice were kindly provided by Dr. Warren Alexander, Walter and Eliza Hall Institute of Medical Research, Australia. CD45.1-congenic OT-I mice were obtained by crossing OT-I mice expressing a transgenic TCR specific for the ovalbumin peptide $OVA_{257-264}$ bound to K^b (kindly provided by Prof. F. Carbone, Melbourne University, Australia) to B6.SJL-Ptrprca (CD45.1$^+$) mice in house. TAP1 KO mice [24] on a C57BL/6 background were originally

obtained from the Walter and Eliza Hall Institute of Medical Research. Animals were monitored daily during experiment and sacrificed by cervical dislocation. All experimental procedures were approved by the Victoria University of Wellington Animal Ethics Committee.

Tumor cell lines and tumor challenge

The B16-F1 murine melanoma (American Type Culture Collection, ATCC) and B16.OVA melanoma expressing a truncated OVA protein [25] were maintained in complete IMDM as described [26]. Extended *in vitro* passaging was avoided for all cell lines. For tumor challenge, cells were washed 3 times in PBS and $2x10^5$ tumor cells were suspended in 100μl of PBS and injected *s.c*. into the flank of mice. Groups of 5 mice were used in most experiments unless otherwise specified. Tumor size and survival were calculated as described [26] and mice culled when tumor reached $150mm^2$.

Immunotherapy treatment

Mice were treated with 50μg Poly I:C (InvivoGen) or 20μg LPS (Sigma) in a total volume of 100μl PBS injected *s.c* around the palpable tumor, at the times indicated. Control mice received 100μl vehicle alone (PBS, Invitrogen). Non-bearing tumor mice were treated *s.c*. with Poly I:C (50μg) for 24h to assess DC maturation state.

Analysis of uric acid levels

C57BL/6J or PLT2 mice were bled by cheek puncture and blood was collected in microtubes containing 5μl of EDTA. After 20 min of centrifugation at 14 000 rpm, plasma was stored in micro tubes at -70˚C. Uric acid levels were measured using Uric Acid Assay Kit (Cayman Chemical).

Flow cytometry

LN and tumors were digested using DNase I and Liberase TL (Roche) and passed through 70μm cells strainers (BD Biosciences) to obtain single cell suspensions. Cells were then resuspended in FACS buffer (PBS with 10mM EDTA, Sigma; 2% FBS, Gibco; and 0.01% NaN_3, Sigma) and blocked with anti-mouse CD16/32 (2.4G2) before staining with combinations of the following antibodies: CD45 (30-F11), CD45.1 (A20), CD3 (145-2C11), CD8α (53–6.7), CD11b (M1/70) and Ly6G (1A8), all from BD Biosciences; CD45 (30-F11), MHCII (M5/114.15.2), Ly6C (HK1.4) and NK1.1 (PK136) from Biolegend; CD45R (RA3-6B2), CD3 (145-2C11), and F4/80 (BM8) from eBioscience and Ly6B (7/4) from AbD Serotec. CD8 (2.43) and CD11c (N418) were affinity purified from hybridoma supernatant. Dead cells were excluded as staining positive for 4',6-diamidino-2-phenylindole (DAPI) or Live/Dead Fixable blue (Invitrogen). For intracellular cytokine staining of T cells, cell suspensions were incubated for 6h at 37˚C in 1μg/ml Golgi Stop (BD Biosciences) and human recombinant IL-2 (in house, 10^2U/ml) with anti-CD3 (5μg/ml) and anti-CD28 (2μg/ml) restimulation. Cells were first stained for surface markers, followed by intracellular staining with anti-IFNγ (BD Biosciences) antibody or isotype control using BD Cytofix/Cytoperm kit (BD Biosciences). Flow cytometry data was acquired using a BD LSRII or a BD LSRFortessa (Beckton Dickinson) and data were analyzed using FlowJo version 9.9. Representative gating is shown in S1 Fig.

Assessment of NK cell cytotoxicity *in vivo*

Mice were injected i.v. with 100μg Poly I:C or PBS as a control. Thirty-six hours later, mice were injected with a 1:1 mixture of CFSE-labelled C57BL/6 and CTO-labelled TAP KO target

spleen cells, as described [27]. Mice were euthanized 6h later and the proportion of CFSE and CTO-labelled cells in spleen was determined by flow cytometry. Percent killing was calculated according to the following formula: 100-[(CTO target / CFSE target in test sample)/(CTO target / CFSE target before injection)]*100.

In vivo T cell proliferation

$CD8^+$ T cells from spleens and LNs of OT-I mice were positively selected using Mouse CD8 FlowComp Dynabeads (Invitrogen) and labeled with CFSE, as described [28]. Flow cytometry analysis confirmed >90% purity as assessed by positive staining with CD8α, Vα2 and Vβ5 antibodies. 1–2 $x10^6$ cells were injected *i.v* into C57BL/6J or PLT2 mice bearing established day 8 B16.OVA tumors. Mice were treated with Poly I:C the following day and OT-I proliferation was assessed in tumor-dLN 3 days later by evaluating CFSE dilution.

Analysis of serum cytokines

Peripheral blood was collected 3h after the first peritumoral treatment and left to clot overnight (16h) at 4˚C. Serum was separated by centrifugation, and cytokines were measured using a custom pre-mixed Millipore Mouse Cytokine Magnetic Bead Panel kit and a Bio-Plex reader (Bio-Rad), according to the manufacturer's instructions.

Statistics

Statistical analyses were performed using Prism 7.0 software (GraphPad). Means ± SEM are shown in all graphs. Tumor survival data were analyzed using the log-rank test with the Bonferroni correction. In all other cases, data were analyzed using two-way ANOVA with Bonferroni correction unless otherwise specified.

Results

Poly I:C tumor immunotherapy is ineffective in PLT2 mice

We tested the impact of the point mutation in the gene encoding for HIU-H on the efficacy of tumor immunotherapy in C57BL/6 wild-type (WT) and PLT2 mice challenged with B16-F1 melanoma. Tumor growth and survival were comparable for WT and PLT2 PBS-treated control mice but, where Poly I:C treatment delayed tumor growth and extended survival in WT mice, Poly I:C treatment had no effect in tumor-bearing PLT2 mice (Fig 1A and 1B).

Consistent with impaired HIU-H function, PLT2 mice exhibited elevated serum uric acid levels compared with sex and age-matched WT mice (Fig 2A). As uric acid has been linked to elevated inflammatory responses, we also compared the effect of Poly I:C treatment on serum cytokine levels in tumor-bearing WT and PLT2 mice. Although Poly I:C treatment did raise the levels of IL-6, MCP-1 and TNFα, there were no significant differences between WT and PLT2 mice (Fig 2B).

Poly I:C-treatment induces DC activation in PLT2 mice

We examined DC populations in the tumor-draining LN (dLN) and tumors of WT and PLT2 mice. As shown in Fig 3A and S2 Fig, Poly I:C treatment caused a similar increase in the number of total $CD11c^+$ $MHCII^+$ DC in the dLN of WT and PLT2 mice. Further DC analysis in WT and PLT2 mice showed no differences in the numbers of $CD11b^+$, $CD103^+$, $CD8^+$ or monocyte-derived DC (moDC) subpopulations. Analysis of the same DC populations in tumors also showed no differences between WT and PLT2 mice (Fig 3B).

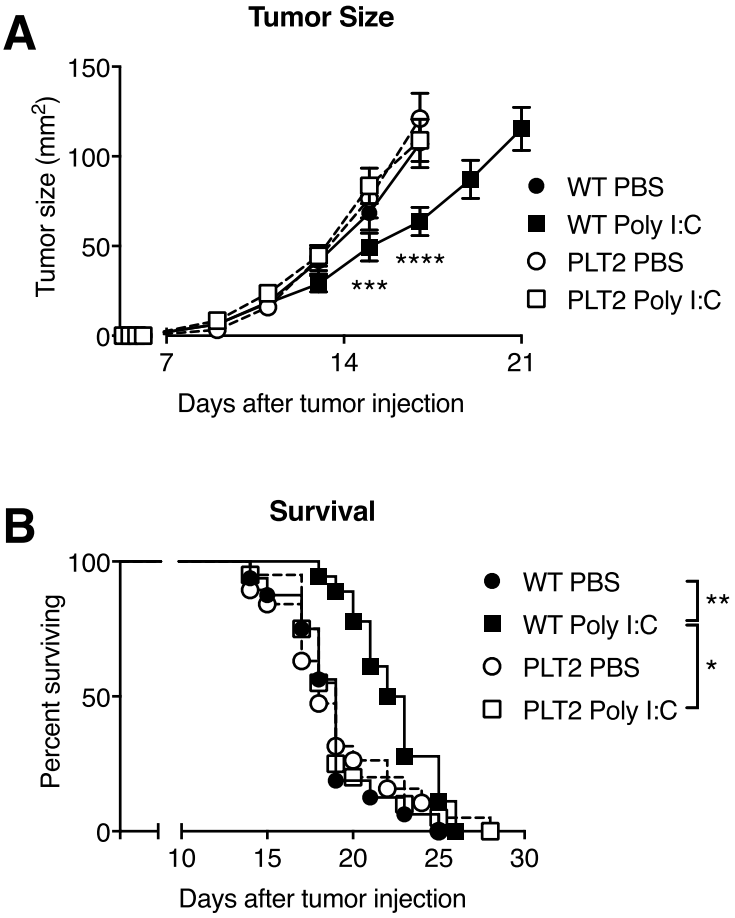

Fig 1. Poly I:C immunotherapy is ineffective in hyperuricaemic PLT2 mice. C57BL/6 (WT) and PLT2 mice were challenged with B16 tumor cells and given peri-tumoral injections of PBS or Poly I:C on days 9, 11, 13 and 15. (**A**) Tumor growth. Graph shows mean tumor size±SEM in groups of 15 mice pooled from three independent experiments. Statistical analysis was by 2-way ANOVA with Tukey's correction, the p values shown in Figure refer to the comparison between WT Poly I:C and PLT2 Poly I:C. $^{***}p<0.001$, $^{****}p<0.0001$. (**B**) Kaplan-Meier survival curves. Data are pooled from four independent experiments, n = 20 mice/group. Statistical analysis was by log-rank test with Bonferroni correction; $^{*}p<0.05$, $^{**}p<0.01$.

https://doi.org/10.1371/journal.pone.0206827.g001

We have reported previously that Poly I:C tumor immunotherapy is associated with increased moDC in the dLN of tumor-bearing mice [21]. As PLT2 and WT mice exhibited comparable changes in DC populations following Poly I:C treatment, we examined phenotypic markers (CD86, CD40, MHCII) linked to DC immune function that might be differentially affected in Poly I:C-treated PLT2 mice. LPS treatment was also included as an immunotherapy negative control [21]. As expected, Poly I:C treatment elevated the number of total DC, $CD11b^+$ DC, $CD103^+$ DC and moDC in the dLN (S3A Fig) while LPS was ineffective. Flow cytometry analysis of the $CD11b^+$ and $CD103^+$ DC and moDC populations showed similar CD86 and CD40 expression on DC from WT and PLT2 mice (S3B Fig), suggesting similar DC responses to immunotherapy.

Poly I:C immunotherapy primes $CD8^+IFN\gamma^+$ T cells in PLT2 mice

We have shown previously that the anti-tumor effect of Poly I:C requires $CD8^+$ T cells [21], and that IFNγ production by $CD8^+$ T cells is essential for anti-tumor activity [29]. As shown in Fig 4A, WT and PLT2 mice showed similar increases in $CD8^+$ T cells in both tumor-dLN and

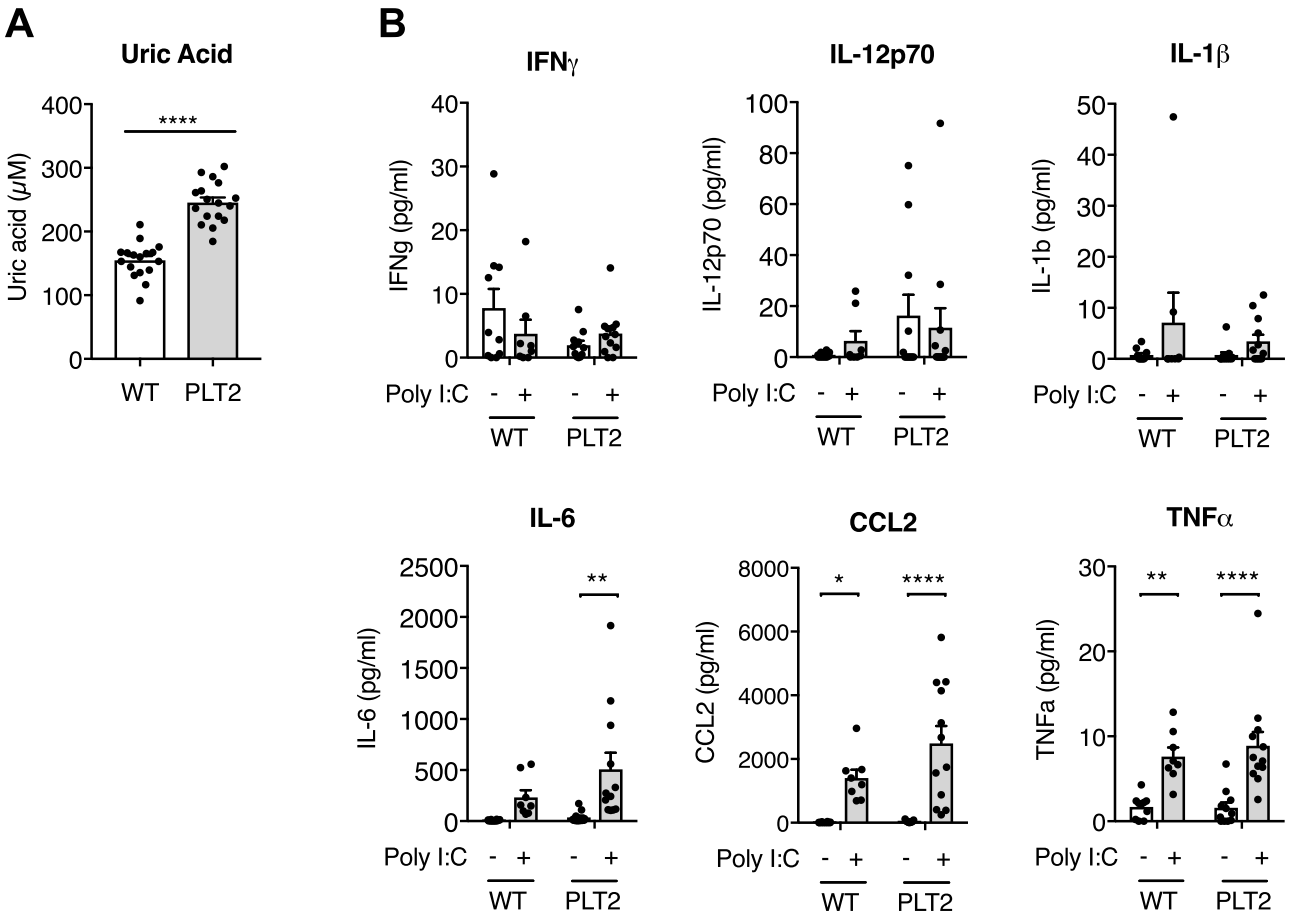

Fig 2. Poly I:C immunotherapy induces serum cytokine responses in both C57BL/6 and PLT2 mice. (**A**) Uric acid levels in untreated C57BL/6 (WT) and PLT2 mice. Mice were gender and age-matched between groups. The bar graph shows mean±SEM for 11 females and 9 males/group, ranging between 9 and 13 weeks of age. Each dot corresponds to one mouse. Statistical analysis was by Mann-Whitney test with ranks comparison, $^{****}p<0.0001$. (**B**) C57BL/6 and PLT2 mice were challenged with B16 tumors and treated with PBS or Poly I:C on day 9. Serum samples were collected three hours later. Cytokine levels were measured by a multiplex bead assay. Bar graphs show the mean+SEM of pooled data from two independent experiments for a total of 8–12 mice/group; each dot corresponds to one mouse. Statistical analysis was by two-way ANOVA with Bonferroni's post-test. $^{*}p<0.05$, $^{**}p<0.01$, $^{****}p<0.0001$.

https://doi.org/10.1371/journal.pone.0206827.g002

tumors. In addition, the proportion of $CD8^+$ T cells producing IFNγ in tumors from WT and PLT2 mice were both increased after Poly I:C immunotherapy compared to control (Fig 4B). The proportions of $CD8^+IFN\gamma^+$ T cells in the tumor immune infiltrate were also increased in Poly I:C-treated WT and PLT2 mice (Fig 4C).

Besides promoting DC activation and $CD8^+$ T cell responses, Poly I:C is a strong inducer of NK cell anti-tumor activity [30]. NK cell numbers in the tumor-dLN of WT and PLT2 mice were increased after Poly I:C immunotherapy, and this increase was more marked in WT compared to PLT2 (S4A Fig). Conversely, a trend to increased proportions of NK cells after Poly I:C immunotherapy was apparent in tumors and reached statistical significance only in PLT2 mice (S4A Fig) In addition, Poly I:C treatment elicited similar *in vivo* NK cell-mediated cytotoxic activity in non tumor-bearing mice (S4B Fig).

The proliferation of tumor-specific $CD8^+$ T cells is increased in PLT2 mice

To investigate further the antigen-specific T cell response to tumor antigen, CSFE-labelled OVA-specific OT-I T cells were adoptively transferred into mice bearing B16-OVA tumors,

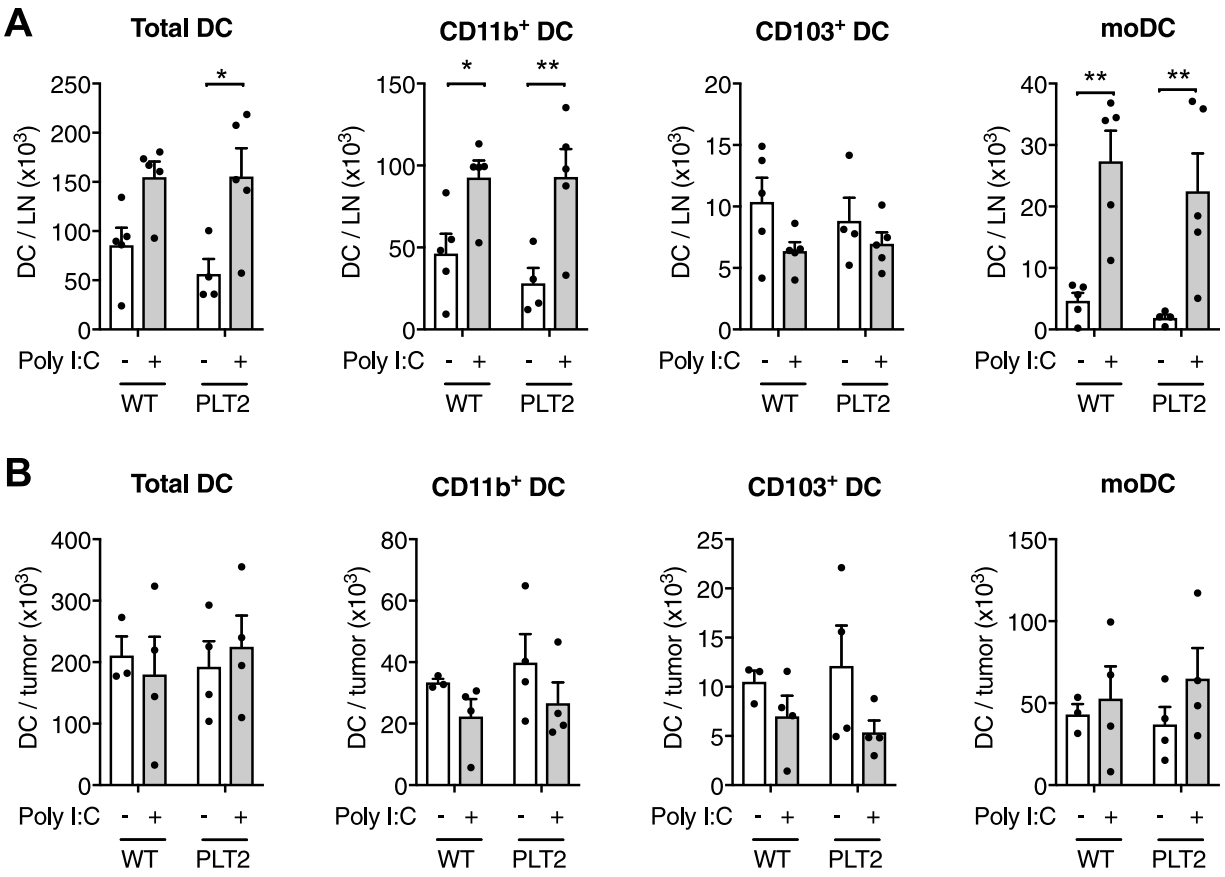

Fig 3. Poly I:C immunotherapy similarly increases DC numbers in the tumor-dLN and tumor of C57BL/6 and PLT2 mice. C57BL/6 (WT) and PLT2 mice were challenged with B16 tumor cells and treated with peri-tumoral injections of PBS or Poly I:C on days 9, 11, 13 and 15. On day 17 the tumors and tumor-dLN were removed and analyzed by flow cytometry using the gating strategy shown in S1 Fig. (**A**) Numbers of total DC ($CD11c^+MHCII^+$), $CD11b^+$ DC ($CD11c^+MHCII^+CD11b^+$ $CD103^-CD8^-Ly6C^-Ly6B^-$), $CD103^+$ DC ($CD11c^+MHCII^+CD11b^-$) and monocyte-derived DC ($CD11c^+MHCII^+CD11b^+Ly6C^+Ly6B^+$) per LN. (**B**) Numbers of the same DC subsets in tumors. Bar graphs show mean +SEM for one of three independent experiments, each with 3–5 mice/group, that gave similar results. Each dot corresponds to one mouse. Statistical analysis was by two-way ANOVA with Bonferroni's post-test, $^*p<0.05$, $^{**}p<0.01$.

https://doi.org/10.1371/journal.pone.0206827.g003

and the effect of Poly I:C treatment on OT-I T cell proliferation in the dLN of WT and PLT2 mice was evaluated (Fig 5A).

As shown in Fig 5B there was a greater proportion of OT-I T cells in the $CD8^+$ T cell population in the dLN compared to the non-dLN of tumor-bearing mice, with a higher proportion of OT-I T cells in the WT compared to PLT2 mice. Poly I:C treatment did not affect the proportion of OT-I T cells in the total $CD8^+$ T cell population. Analysis of OT-I T cell proliferation by CFSE dilution showed more proliferation of OT-I T cells in the dLN and non-dLN of PLT2 mice than in WT mice (Fig 5A and 5C–5E). There were significantly fewer undivided OT-I T cells in PLT2 compared to WT mice in both the dLN and non-dLN of tumor-bearing mice (Fig 5A and 5C). There were also fewer undivided cells in the dLN compared to the non-dLN in both PLT2 and WT mice. Moreover, there was a trend of decreased undivided cells with Poly I:C treatment in both PLT2 and WT mice.

Consistent with the pattern for undivided OT-I T cells, we observed a greater proportion of divided and highly divided OT-I T cells in the dLN and non-dLN of tumor-bearing PLT2 mice compared to WT mice (Fig 5A, 5D and 5E). Whereas Poly I:C treatment had little effect on OT-I T cells in non-dLN, there was a trend towards more divided and highly divided OT-I T

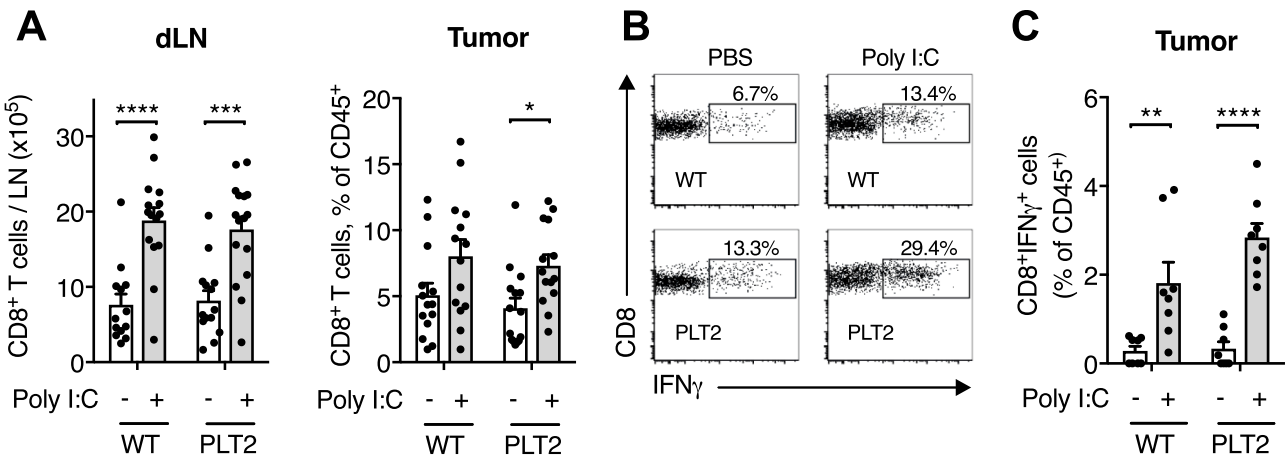

Fig 4. Poly I:C immunotherapy increases the proportion of intratumoral CD8$^+$IFNγ$^+$ T cells in C57BL/6 and PLT2 mice. C57BL/6 (WT) and PLT2 mice were challenged with B16 tumor cells and treated with peri-tumoral injections of PBS or Poly I:C on day 9, 11, 13 and 15. On day 17, tumor-dLN and tumors were removed for flow cytometry analysis. (**A**) Total numbers of CD8$^+$ T cells in dLN and tumors. (**B**) Representative flow plots showing the proportion of IFNγ$^+$ cells in the intratumoral CD8$^+$ T cell population as determined by intracellular cytokine staining. (**C**) Proportions of CD8$^+$IFNγ$^+$ cells in tumors, expressed as percentage of the CD45$^+$ population. Bar graphs show mean+SEM for pooled data from 2–5 independent experiments, each with 4–5 mice/group, that gave similar results. Each dot refers to one mouse. Statistical analysis was by two-way ANOVA with Bonferroni's post-test. $^*p<0.05$, $^{**}p<0.01$, $^{***}p<0.001$, $^{****}p<0.0001$.

https://doi.org/10.1371/journal.pone.0206827.g004

cells in the dLN of both PLT2 and WT mice, with the greatest impact on OT-I T cells in WT mice.

Discussion

There is increasing evidence of MS and hyperuricaemia contributing to poor outcomes in cancer [1, 2, 9, 14]. In this study we used PLT2 mice that offer the benefit of stable hyperuricemia without the concomitant effects of drug-induced hyperuricemia models [31]. We found that dysfunctional purine metabolism caused elevated serum uric acid levels in PLT2 mice and negatively impacted on the effectiveness of Poly I:C immunotherapy to delay tumor growth in a subcutaneous model of B16 melanoma.

Clinical studies indicate that MS and hyperuricaemia may increase the incidence of some cancers such as colorectal cancer [4, 10]. PLT2 mice also show a predisposition to developing hepatocarcinoma over time [18]. In comparison, our findings showed growth of B16 tumors to be similar in both control WT and PLT2 mice. It is possible that the more acute nature of the B16 tumor model overrides the long-term effect of chronic purine metabolic dysfunction on tumor development and growth observed in other studies. The type of cancer as well as the site of tumor induction, skin versus liver, may also play a role.

Our data identify that disruption of purine metabolism alters the efficacy of the anti-tumor immunotherapy Poly I:C. It is postulated that elevated uric acid levels is a surrogate indicator of an inflammatory environment that favors tumorigenesis and enables tumor growth [14, 32, 33]. We did not observe any significant differences in the inflammatory cytokine profiles in the blood of tumor-bearing WT and PLT2 mice regardless of whether they received treatment with the anti-tumor agent Poly I:C. Serum levels of type I IFN were not measured in these experiments, but the similar DC activation profile in C57BL/6 and PLT2 mice, which is IFN-I-dependent [34], suggests no major defects in the production of this cytokine. As such it does not appear that differences in classical inflammatory cytokines contribute to the observed loss of anti-tumor activity in the PLT2 mice.

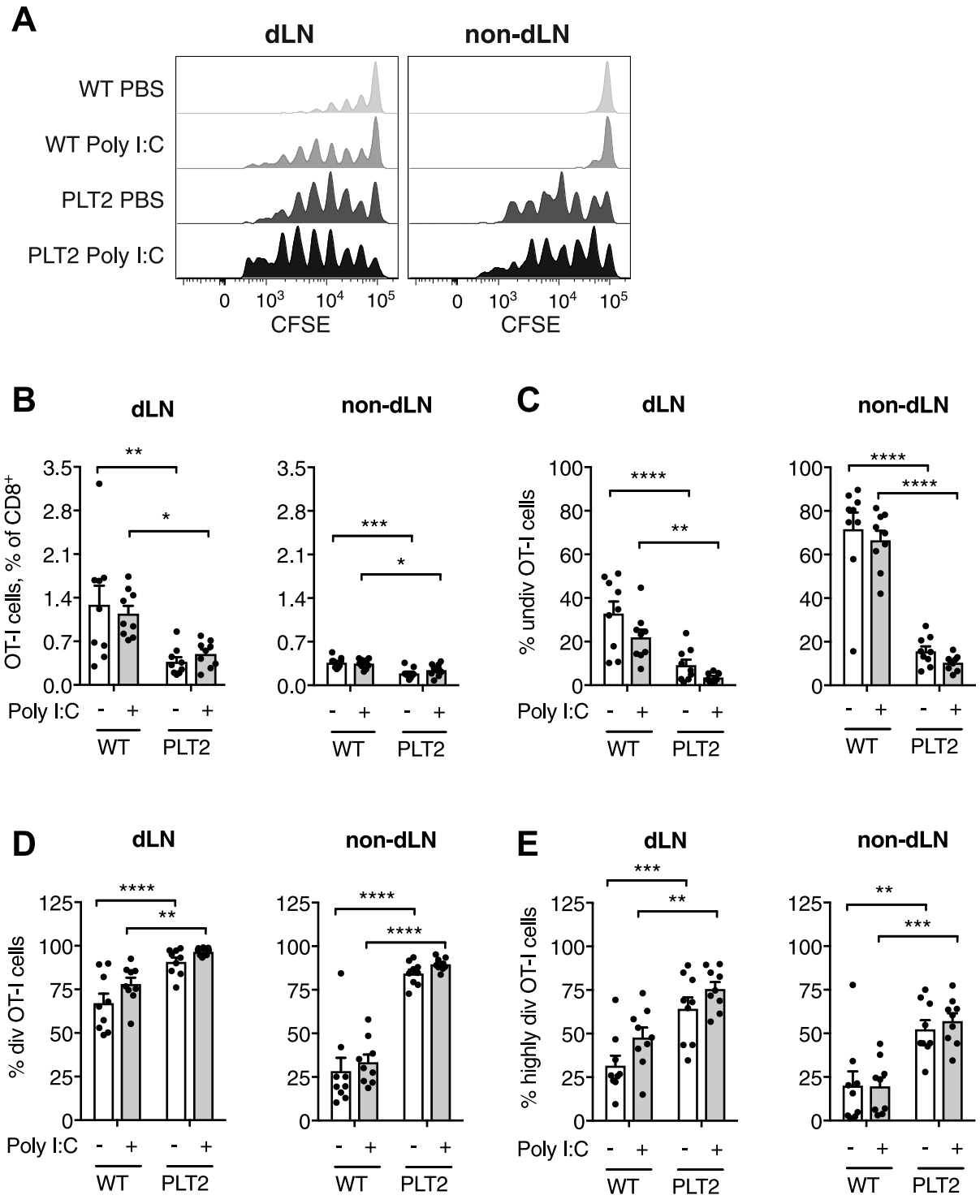

Fig 5. Tumor-specific CD8$^+$ T cells proliferate more vigorously in PLT2 than C57BL/6 mice irrespective of Poly I:C immunotherapy. C57BL/6 (WT) and PLT2 mice were challenged with B16.OVA tumor cells. CFSE-labelled OT-I T cells were adoptively transferred into tumor-bearing mice on day 8. Mice were treated with peri-tumoral injections of Poly I:C or PBS on day 9, and tumor-dLN were removed on day 12 for flow cytometry analysis. (**A**) Representative histograms of OT-I T cells in tumor-draining and contralateral LN. OT-I T cells were identified as CD8$^+$CD45.1$^+$. (**B**) Proportion of OT-I T cells in the CD8$^+$ T cell population in draining and non-dLN. (**C-E**) Proportions of undivided, divided, and highly divided (4 or more divisions) OT-I T cells in draining and non-draining LN. Bar graphs show mean+SEM for pooled data from two independent experiments each with 4–5 mice/group. Each dot refers to one mouse. Statistical analysis was by two-way ANOVA with Bonferroni's post-test. $^*p<0.05$, $^{**}p<0.01$, $^{***}p<0.001$, $^{****}p<0.0001$.

https://doi.org/10.1371/journal.pone.0206827.g005

Antigen presenting cells, most commonly DC, are widely recognized as playing a pivotal role in raising anti-tumor responses in the treatment of cancer. Previous work on the adjuvant effects of crystalline monosodium urate (MSU) and mycobacteria in boosting cancer immunotherapy also points towards monocyte derived DC in orchestrating beneficial anti-tumor activity [21]. It is also proposed that soluble uric acid has the ability to enhance DC function [35, 36]. Our data showed no such enhanced activation of DC populations in hyperuricaemic PLT2 mice compared with WT in the steady-state, and no increased response to treatment with Poly I:C or LPS.

The expansion and activation of NK cells and antigen-specific IFNγ-producing $CD8^+$ T cells are common targets for effective anti-tumor activity [19, 20]. In this study WT and PLT2 mice exhibited similar profiles for NK cells and for total $CD8^+$ T cells as well as $CD8^+IFN\gamma^+$ T cells, indicating that the NK and $CD8^+$ T cell phenotype might not be involved in the loss of anti-tumor activity in the PLT2 mice. However, closer inspection of the antigen-specific response indicated a significantly smaller proportion of antigen-specific $CD8^+$ T cells present in PLT2 mice.

It has been reported that uric acid plays a key role in boosting $CD8^+$ T cell responses in transplant and diabetes models including enhanced $CD8^+$ T cell proliferation [35, 37]. It is therefore notable that PLT2 mice exhibited a greater proportion of proliferating antigen-specific OT-I T cells in both draining and non-draining LNs, before and after Poly I:C treatment, compared to WT mice without translating into better anti-tumor activity. The relationship between the increased proliferation of tumor-specific $CD8^+$ T cells and their decreased proportion in the tumor-dLN of PLT2 mice remains unclear and may suggest that these highly divided cells were not surviving well in PLT2 hosts. It is also possible that this high background proliferation in the PLT2 mice might limit the ability of the Poly I:C treatment to further expand the antigen specific $CD8^+$ T cell population sufficiently to raise an effective anti-tumor immune response.

Our findings introduce the concept that chronic dysfunctional purine metabolism and hyperuricaemia could in some cases compromise anticancer therapy. This may be particularly relevant in situations where cancer treatment results in extensive tissue/cell death leading to highly elevated uric acid levels. A number of urate-lowering therapies are already used in cancer treatment—primarily to control Tumor Lysis Syndrome. The potential for managing purine metabolism and uric acid as a means to improve anti-cancer therapy warrants further investigation.

Supporting information

S1 Fig. Gating of DC subsets. Flow cytometry gating used to define DC subsets in LN. (**A**) Conventional DC (cDC) were $CD11c^+MHCII^+$; $CD11b^+$ DC were $CD11c^+MHCII^+CD11b^+$ $CD103^-CD8^-Ly6C^-Ly6B^-$; $CD8^+$ DC were $CD11c^+MHCII^+CD11b^-$; $CD103^+$ DC were $CD11c^+MHCII^+CD11b^-$. (**B**) monocyte-derived DC (moDC) were $CD11c^+MHCII^+Ly6C^+Ly6B^+$ and expressed high CD11b (not shown).
(EPS)

S2 Fig. Poly I:C immunotherapy increases DC numbers in the tumor-dLN of C57BL/6 and PLT2 mice. C57BL/6 (WT) and PLT2 mice were challenged with B16 tumor cells and treated with peri-tumoral injections of PBS or Poly I:C on days 9, 11, 13 and 15. On day 17 the tumor-dLN were removed and analyzed by flow cytometry. DC gating was as shown in S1 Fig. Numbers of total "conventional" DC, $CD11b^+$ DC, $CD8^+$ DC and monocyte-derived DC per LN. Bar graphs show mean and SEM for two combined experiments, each with 3–5 mice/group. Each dot corresponds to one mouse. Statistical analysis was by two-way ANOVA with

Bonferroni's post-test, $^{*}p<0.05$, $^{**}p<0.01$, $^{***}p<0.001$.
(EPS)

S3 Fig. Effect of Poly I:C or LPS treatment on DC numbers and surface marker expression in PLT2 and WT mice. C57BL/6 (WT) and PLT2 mice were injected with PBS, LPS or poly I:C into the flank, and dLN were harvested 24h later for flow cytometry analysis. (**A**) Number of total DC, $CD11b^{+}$ DC, $CD103^{+}$ DC and moDC per LN. DC subsets were identified as in Fig 3. Data are pooled from three independent experiments, each with 3–4 mice/group, that gave similar results. Bar graphs show mean+SEM, each dot corresponds to one mouse. Statistical analysis was by two-way ANOVA with Bonferroni's post-test; $^{***}p<0.001$, $^{****}p<0.0001$. (**B**) Surface expression of the activation markers CD40 and CD86 on the indicated DC subsets; representative samples from one experiment are shown.
(EPS)

S4 Fig. Poly I:C immunotherapy increases the frequency of NK cells in the tumor-dLN of WT and PLT2 mice, and their cytotoxic activity. (**A**): Mice were treated with PBS or Poly I:C at the tumor site and euthanized after 4 treatments. NK cell numbers in tumor-dLN, and their frequencies in tumors, were calculated using flow cytometry. Data are pooled from three independent experiments, each with 3–5 mice per group. (**B**): Mice were treated intravenously with PBS or Poly I:C. Thirty-six hours later, mice were injected with a mixture of TAP KO and WT labeled splenocytes, and the relative proportion of TAP KO cells compared to WT was assessed 6h later to estimate killing. Data are pooled from two independent experiments each with three mice/group. Bar graphs show mean+SEM, each dot corresponds to one mouse. Statistical analysis was by two-way ANOVA with Bonferroni's post-test; $^{*}p<0.05$, $^{**}p<0.01$, $^{****}p<0.0001$.
(EPS)

Acknowledgments

The authors wish to thank the expert support of the Malaghan Institute of Medical Research Hugh Green Cytometry Core and Biomedical Research Unit staff.

Author Contributions

Conceptualization: Franca Ronchese, Jacquie L. Harper.

Formal analysis: Camille Baey, Jianping Yang.

Funding acquisition: Franca Ronchese, Jacquie L. Harper.

Investigation: Camille Baey, Jianping Yang.

Writing – original draft: Camille Baey, Jacquie L. Harper.

Writing – review & editing: Camille Baey, Jianping Yang, Franca Ronchese, Jacquie L. Harper.

References

1. Esposito K, Chiodini P, Colao A, Lenzi A, Giugliano D. Metabolic syndrome and risk of cancer: a systematic review and meta-analysis. Diabetes Care. 2012; 35(11):2402–11. Epub 2012/10/25. https://doi.org/10.2337/dc12-0336 PMID: 23093685.
2. Mendonca FM, de Sousa FR, Barbosa AL, Martins SC, Araujo RL, Soares R, et al. Metabolic syndrome and risk of cancer: which link? Metabolism. 2015; 64(2):182–9. Epub 2014/12/03. https://doi.org/10.1016/j.metabol.2014.10.008 PMID: 25456095.

3. Micucci C, Valli D, Matacchione G, Catalano A. Current perspectives between metabolic syndrome and cancer. Oncotarget. 2016; 7(25):38959–72. Epub 2016/10/23. https://doi.org/10.18632/oncotarget.8341 PMID: 27029038.
4. Esposito K, Chiodini P, Capuano A, Bellastella G, Maiorino MI, Rafaniello C, et al. Colorectal cancer association with metabolic syndrome and its components: a systematic review with meta-analysis. Endocrine. 2013; 44(3):634–47. Epub 2013/04/03. https://doi.org/10.1007/s12020-013-9939-5 PMID: 23546613.
5. Ishino K, Mutoh M, Totsuka Y, Nakagama H. Metabolic syndrome: a novel high-risk state for colorectal cancer. Cancer Lett. 2013; 334(1):56–61. Epub 2012/10/23. https://doi.org/10.1016/j.canlet.2012.10.012 PMID: 23085010.
6. Gacci M, Russo GI, De Nunzio C, Sebastianelli A, Salvi M, Vignozzi L, et al. Meta-analysis of metabolic syndrome and prostate cancer. Prostate Cancer Prostatic Dis. 2017; 20(2):146–55. Epub 2017/02/22. https://doi.org/10.1038/pcan.2017.1 PMID: 28220805.
7. Bhandari R, Kelley GA, Hartley TA, Rockett IR. Metabolic syndrome is associated with increased breast cancer risk: a systematic review with meta-analysis. Int J Breast Cancer. 2014; 2014:189384. Epub 2015/02/06. https://doi.org/10.1155/2014/189384 PMID: 25653879.
8. Hauner D, Hauner H. Metabolic syndrome and breast cancer: is there a link? Breast Care (Basel). 2014; 9(4):277–81. Epub 2014/11/19. https://doi.org/10.1159/000365951 PMID: 25404888.
9. Esposito K, Capuano A, Giugliano D. Metabolic syndrome and cancer: holistic or reductionist? Endocrine. 2014; 45(3):362–4. Epub 2013/09/26. https://doi.org/10.1007/s12020-013-0056-2 PMID: 24065310.
10. Kim HJ, Kim JE, Jung JH, Kim ER, Hong SN, Chang DK, et al. Uric Acid Is a Risk Indicator for Metabolic Syndrome-related Colorectal Adenoma: Results in a Korean Population Receiving Screening Colonoscopy. Korean J Gastroenterol. 2015; 66(4):202–8. Epub 2015/10/24. https://doi.org/10.4166/kjg.2015.66.4.202 PMID: 26493505.
11. Lima WG, Martins-Santos ME, Chaves VE. Uric acid as a modulator of glucose and lipid metabolism. Biochimie. 2015; 116:17–23. Epub 2015/07/03. https://doi.org/10.1016/j.biochi.2015.06.025 PMID: 26133655.
12. Olson OC, Quail DF, Joyce JA. Obesity and the tumor microenvironment. Science. 2017; 358 (6367):1130–1. Epub 2017/12/02. https://doi.org/10.1126/science.aao5801 PMID: 29191893.
13. Simpson ER, Brown KA. Obesity and breast cancer: role of inflammation and aromatase. J Mol Endocrinol. 2013; 51(3):T51–9. Epub 2013/10/29. https://doi.org/10.1530/JME-13-0217 PMID: 24163427.
14. Fini MA, Elias A, Johnson RJ, Wright RM. Contribution of uric acid to cancer risk, recurrence, and mortality. Clin Transl Med. 2012; 1(1):16. Epub 2013/02/02. https://doi.org/10.1186/2001-1326-1-16 PMID: 23369448.
15. Chen CJ, Yen JH, Chang SJ. Gout patients have an increased risk of developing most cancers, especially urological cancers. Scand J Rheumatol. 2014; 43(5):385–90. Epub 2014/05/16. https://doi.org/10.3109/03009742.2013.878387 PMID: 24825466.
16. Wang W, Xu D, Wang B, Yan S, Wang X, Yin Y, et al. Increased Risk of Cancer in relation to Gout: A Review of Three Prospective Cohort Studies with 50,358 Subjects. Mediators Inflamm. 2015; 2015:680853. Epub 2015/10/28. https://doi.org/10.1155/2015/680853 PMID: 26504360.
17. Baldwin W, McRae S, Marek G, Wymer D, Pannu V, Baylis C, et al. Hyperuricemia as a mediator of the proinflammatory endocrine imbalance in the adipose tissue in a murine model of the metabolic syndrome. Diabetes. 2011; 60(4):1258–69. Epub 2011/02/25. https://doi.org/10.2337/db10-0916 PMID: 21346177.
18. Stevenson WS, Hyland CD, Zhang JG, Morgan PO, Willson TA, Gill A, et al. Deficiency of 5-hydroxyisourate hydrolase causes hepatomegaly and hepatocellular carcinoma in mice. Proc Natl Acad Sci U S A. 2010; 107(38):16625–30. Epub 2010/09/09. https://doi.org/10.1073/pnas.1010390107 PMID: 20823251.
19. Melief CJ, van Hall T, Arens R, Ossendorp F, van der Burg SH. Therapeutic cancer vaccines. J Clin Invest. 2015; 125(9):3401–12. Epub 2015/07/28. https://doi.org/10.1172/JCI80009 PMID: 26214521.
20. Smyth MJ, Ngiow SF, Ribas A, Teng MW. Combination cancer immunotherapies tailored to the tumour microenvironment. Nat Rev Clin Oncol. 2016; 13(3):143–58. Epub 2015/11/26. https://doi.org/10.1038/nrclinonc.2015.209 PMID: 26598942.
21. Kuhn S, Hyde EJ, Yang J, Rich FJ, Harper JL, Kirman JR, et al. Increased numbers of monocyte-derived dendritic cells during successful tumor immunotherapy with immune-activating agents. J Immunol. 2013. https://doi.org/10.4049/jimmunol.1301135 PMID: 23858033
22. Steiger S, Kuhn S, Ronchese F, Harper JL. Monosodium Urate Crystals Induce Upregulation of NK1.1-Dependent Killing by Macrophages and Support Tumor-Resident NK1.1+ Monocyte/Macrophage

Populations in Antitumor Therapy. J Immunol. 2015; 195(11):5495–502. Epub 2015/11/04. https://doi.org/10.4049/jimmunol.1401755 PMID: 26525286.

23. Caravaca-Fontan F, Martinez-Saez O, Pampa-Saico S, Olmedo ME, Gomis A, Garrido P. Tumor lysis syndrome in solid tumors: Clinical characteristics and prognosis. Med Clin (Barc). 2017; 148(3):121–4. Epub 2016/12/21. https://doi.org/10.1016/j.medcli.2016.10.040 PMID: 27993406.

24. Van Kaer L, Ashton-Rickardt P, Ploegh H, Tonegawa S. TAP1 mutant mice are deficient in antigen presentation, surface class I molecules, and CD4-8+ T cells. Cell. 1992; 71(7):1205–14. PMID: 1473153

25. Lugade AA, Moran JP, Gerber SA, Rose RC, Frelinger JG, Lord EM. Local radiation therapy of B16 melanoma tumors increases the generation of tumor antigen-specific effector cells that traffic to the tumor. J Immunol. 2005; 174(12):7516–23. Epub 2005/06/10. PMID: 15944250.

26. Ataera H, Hyde E, Price KM, Stoitzner P, Ronchese F. Murine melanoma-infiltrating dendritic cells are defective in antigen presenting function regardless of the presence of CD4CD25 regulatory T cells. PLoS One. 2011; 6(3):e17515. Epub 2011/03/11. https://doi.org/10.1371/journal.pone.0017515 PMID: 21390236.

27. Hermans I, Silk J, Yang J, Palmowski M, Gileadi U, McCarthy C, et al. The VITAL assay: a versatile fluorometric technique for assessing CTL- and NKT-mediated cytotoxicity against multiple targets *in vitro* and *in vivo*. J Immunol Methods. 2004; 285(1):25–40. https://doi.org/10.1016/j.jim.2003.10.017 PMID: 14871532

28. Ma JZ, Lim SN, Qin JS, Yang J, Enomoto N, Ruedl C, et al. Murine CD4+ T cell responses are inhibited by cytotoxic T cell-mediated killing of dendritic cells and are restored by antigen transfer. PLoS One. 2012; 7(5):e37481. Epub 2012/06/01. https://doi.org/10.1371/journal.pone.0037481 PMID: 22649530.

29. Kemp RA, Ronchese F. Tumor-specific Tc1, but not Tc2, cells deliver protective antitumor immunity. J Immunol. 2001; 167(11):6497–502. Epub 2001/11/21. PMID: 11714817.

30. Oehler J, Lindsay L, Nunn M, Holden H, Herberman R. Natural cell-mediated cytotoxicity in rats. II. *In vivo* augmentation of NK-cell activity. Int J Cancer. 1978; 21(2):210–20. PMID: 627428.

31. Ben Salem C, Slim R, Fathallah N, Hmouda H. Drug-induced hyperuricaemia and gout. Rheumatology. 2017; 56:679–88. https://doi.org/10.1093/rheumatology/kew293 PMID: 27498351

32. Lu W, Xu Y, Shao X, Gao F, Li Y, Hu J, et al. Uric Acid Produces an Inflammatory Response through Activation of NF-kappaB in the Hypothalamus: Implications for the Pathogenesis of Metabolic Disorders. Sci Rep. 2015; 5:12144. Epub 2015/07/17. https://doi.org/10.1038/srep12144 PMID: 26179594.

33. Sangkop F, Singh G, Rodrigues E, Gold E, Bahn A. Uric acid: a modulator of prostate cells and activin sensitivity. Mol Cell Biochem. 2016; 414(1–2):187–99. Epub 2016/02/26. https://doi.org/10.1007/s11010-016-2671-8 PMID: 26910779.

34. Longhi M, Trumpfheller C, Idoyaga J, Caskey M, Matos I, Kluger C, et al. Dendritic cells require a systemic type I interferon response to mature and induce CD4+ Th1 immunity with poly IC as adjuvant. J Exp Med. 2009; 206(7):1589–602. https://doi.org/10.1084/jem.20090247 PMID: 19564349

35. Ma XJ, Tian DY, Xu D, Yang DF, Zhu HF, Liang ZH, et al. Uric acid enhances T cell immune responses to hepatitis B surface antigen-pulsed-dendritic cells in mice. World J Gastroenterol. 2007; 13(7):1060–6. Epub 2007/03/22. https://doi.org/10.3748/wjg.v13.i7.1060 PMID: 17373740.

36. Braga TT, Forni MF, Correa-Costa M, Ramos RN, Barbuto JA, Branco P, et al. Soluble Uric Acid Activates the NLRP3 Inflammasome. Sci Rep. 2017; 7:39884. https://doi.org/10.1038/srep39884 PMID: 28084303.

37. Shi Y, Galusha SA, Rock KL. Cutting edge: elimination of an endogenous adjuvant reduces the activation of CD8 T lymphocytes to transplanted cells and in an autoimmune diabetes model. J Immunol. 2006; 176(7):3905–8. Epub 2006/03/21. PMID: 16547223.